

The compositional and molecular character of the calcium silicate hydrates formed in the paste hydration of $3\text{CaO} \cdot \text{SiO}_2$

E. HENDERSON¹, J. E. BAILEY

Department of Engineering Materials, University of Sheffield, Sheffield, S1 3JD, UK

Transmission electron microscopy has been used to determine the composition and characterize the molecular structure of the early calcium silicate hydrates formed in the paste hydration of $3\text{CaO} \cdot \text{SiO}_2$. The initial surface hydrates were found to have a wide range of CaO/SiO_2 compositions, consistent with the rapid and variable rate of dissolution of Ca^{2+} ions from only specific reactive surface sites. The very early surface hydrates appear disordered on a 1 nm scale. At later ages these become microheterogeneous, with more structurally ordered sheet-like fragments and regions developing within the disordered regions. Discrete 3 nm long and 1 nm thick fragments and more structurally ordered assemblies of these were observed. The basic molecular core structure was found to be a 1 nm thick sheet consisting of a protonated CaO_x polyhedral layer sandwiched between short-chain silicate groups. In these paste hydrates, this layer extends for only 3 nm before disordering recurs.

1. Introduction

The general features of the hydration reaction of Portland cements, and the overall microstructure of the products, have been recognized for many years; however, the detailed mechanism remains uncertain. Portland cements contain up to 80% by weight of the calcium silicate phases, $3\text{CaO} \cdot \text{SiO}_2$ (65%) and $\beta\text{-}2\text{CaO} \cdot \text{SiO}_2$ (15%). On hydration these produce an apparently disordered calcium silicate hydrate of somewhat variable composition, but with a CaO/SiO_2 ratio usually in the range 1.5 to 2.0 and crystalline $\text{Ca}(\text{OH})_2$ [1]. Since the calcium silicates are the predominant phases, their hydration products are of great importance in relation to the overall durability and mechanical behaviour of concrete, mortar, etc. In spite of this the hydration mechanism is not fully understood [1–4] and the micro structural and molecular characteristics of the calcium silicate hydrate are still uncertain [4, 5].

Of particular importance within the overall hydration process is the character of the early hydrolysis reaction between water molecules and anhydrous $3\text{CaO} \cdot \text{SiO}_2$, during the first few minutes and hours. The complex processes occurring within both the initial rapid surface dissolution stage and the subsequent so-called “dormant period” have been studied using a variety of techniques [1, 6–8]. Of particular interest are the thermoluminescence studies of Fierens and Verhaegen [8, 9] into the surface reactivity of $3\text{CaO} \cdot \text{SiO}_2$. These investigations have shown the importance of reactive surface sites in the initial hydration process. These nucleophilic active “defects” in the lattice were found to be preferentially attacked by

water molecules [9, 10]. Surface-sensitive techniques such as X-ray photoelectron spectroscopy (XPS) and electron spectroscopy for chemical analysis (ESCA) have been used to probe the first 2 nm of the hydrating $3\text{CaO} \cdot \text{SiO}_2$ surface [11, 12]. These techniques have shown that the surface CaO/SiO_2 ratio changes with hydration time, falling rapidly within the first few minutes to approximately 2.5, then increasing, before gradually decreasing to a CaO/SiO_2 ratio somewhat below 2 [11, 12]. Although these techniques are capable of analysing the first few nanometres of a surface, their spatial resolution has until more recently been typically 25 nm² for ESCA. The compositional changes described above are therefore surface-averaged values.

As part of the present investigation transmission electron microscopy (TEM) has been used to characterize the early hydration products in the $3\text{CaO} \cdot \text{SiO}_2\text{-H}_2\text{O}$ system. In contrast to the above we will discuss analytical results obtained using the high spatial resolution possible with modern TEM.

The microstructural and molecular character of the calcium silicate hydrate formed in the paste hydration of calcium silicates remains uncertain. Most microstructural and indirect surface area studies indicate a two-dimensional layer-like structure [13–15]. Non-layered structures have however been proposed for both synthetic calcium silicate hydrates and the paste hydrates in Portland cements [16, 17]. The majority of synthetic preparations are generally regarded from X-ray diffraction evidence to have a two-dimensional layer-like structure, reminiscent of the crystal structure of the mineral tobermorite [18–20], the basic

¹ Present address: Euroc Research AB, 22370 Lund, Sweden.

structure of which is based on a CaO_x polyhedral layer sandwiched between long-chain silicate groups [21]. Structural differences that do exist between synthetic hydrates and tobermorite are thought to be mainly related to the difference in chain length [22, 23]. Direct TEM evidence of the layer-like molecular structure reminiscent of tobermorite has been obtained by Henderson and Bailey [24].

The structure of the calcium silicate hydrate formed during the paste hydration of Portland cement still remains uncertain. Taylor [25] has proposed a complex microheterogeneous structure for this hydrate, in which any sub-crystalline order that may exist is confined to the neighbourhood of small fragments of CaO_x layers, only a few nanometres long, and rarely parallel.

In view of the above uncertainties concerning the basic structure of the calcium silicate hydrates and the interesting microheterogeneous structure proposed, we have studied the early hydrates formed in the paste hydration of $3\text{CaO}\cdot\text{SiO}_2$. By using this approach it has been possible to characterize the microstructural and molecular detail within the paste hydrates using TEM.

2. Experimental procedure

The $3\text{CaO}\cdot\text{SiO}_2$ polymorph was prepared by repeated firings at 1450°C , with intermediate grinding, until the free lime content was reduced to 0.5%. The sample was finally ground to an air permeability surface of $0.40\text{ m}^2\text{ g}^{-1}$, with an average particle size of

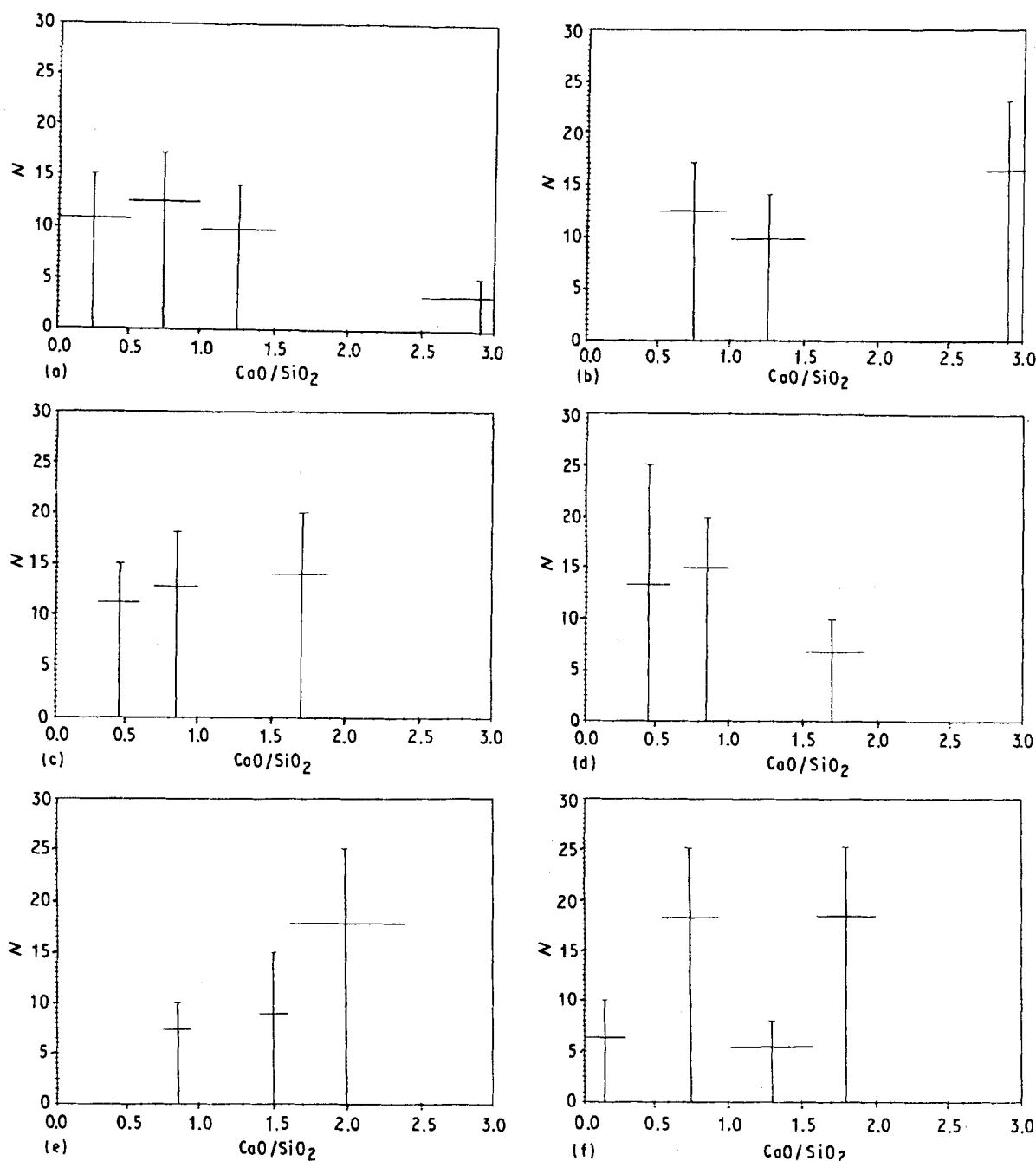


Figure 1 Analytical TEM of surface layers and outgrowths: N = no. of analyses, horizontal bar = standard deviation. Surface layers at 0.5 h with analysis beam (a) 10 nm and (b) 40 nm from surface; (c) surface layers and (d) outgrowths at 3 h (10 nm); (e) surface layers and (f) outgrowths at 3 h (40 nm); (g) surface layers and (h) outgrowths at 7 h (10 nm); (i) surface layers and (j) outgrowths at 7 h (40 nm).

close to 6 μm . The overall hydration at early ages was monitored by conduction calorimetry.

In these investigations the development of the hydrates was studied at four hydration ages, namely at an early stage 0.5 h, during the dormant period at 3 h, during the period of energy release at 7 h and finally at 24 h, after the maximum in the energy release curve. These ages were chosen as representative of the hydration products formed at comparatively low overall degrees of hydration. All the paste mixes used a water ratio of 0.5 and the hydration was stopped by washings with acetone, followed by drying over SiO_2 gel.

For the electron microscope studies, the dried powders were suspended in propan-2-ol, and a capillary drop from each was run on to holey carbon Cu TEM grids. The specimens were examined in axial bright field at 100 keV using a Philips 400T transmission electron microscope. The samples were analysed using a 'thin film' program and pre-determined k factors, using an energy-dispersive X-ray analysis (EDAX) system. Most of the elemental analysis was undertaken using a TEM microprobe spot size of 40 nm. The 10 nm and 40 nm values quoted below are the distances of the inner edge of the spot from the outer surface of the area being analysed. Only those areas of the hydrated $3\text{CaO}\cdot\text{SiO}_2$ surface that were thin enough to obtain a general TEM image were analysed, this being regarded as close to the limit for the above thin film analysis. For the higher resolution images of the surface hydrates thinner regions were selected, by observing the movement and character of the surface as the specimen was tilted.

3. Results and discussion

In this investigation three basic aspects of the initial development and character of the amorphous surface hydrates were studied in some detail. One particular aim was to analyse these hydrates to determine the possible range of CaO/SiO_2 compositional types at early ages, and to elucidate the dynamics of compositional variations through the dormant period to the acceleratory period, when the overall degree of hydration becomes increasingly more significant. In addition, changes in the microstructural and molecular character of these early hydrates were also studied. This in particular follows on from our earlier ca. 1 nm scale imaging of calcium silicate hydrates formed in model systems [24].

3.1. Compositional studies of the early hydrates

To obtain a representative quantitative analysis of the changes in the surface composition of hydrating $3\text{CaO}\cdot\text{SiO}_2$ a large number of individual analyses were undertaken at the three chosen hydration times. In view of the wide range of CaO/SiO_2 ratios determined, the results are plotted for convenience as bar charts in Fig. 1 and the data summarized in Table I. At 0.5 h hydration the analysis was restricted to only the surface layers, i.e. the film edge. At the later ages the hydrated surface was found to have two somewhat different microstructural types which have been termed "surface layers" and "outgrowths". The development of these defined types through the first 24 h hydration is shown schematically in Fig. 2. The plan

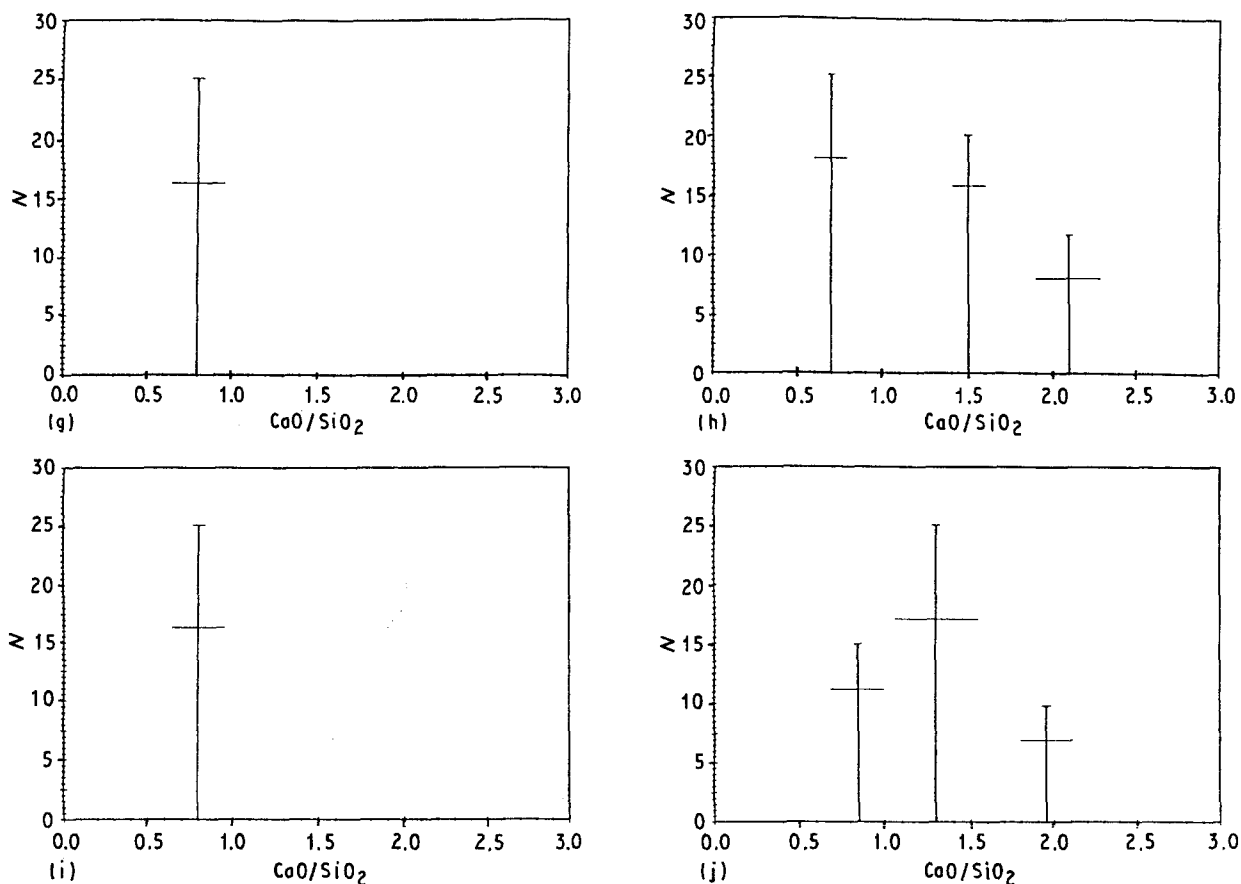


Figure 1 Continued.

TABLE I Analytical TEM of designated calcium silicate hydrate types in the $3\text{CaO}\cdot\text{SiO}_2\text{-H}_2\text{O}$ system at early ages

Hydration age	CaO/SiO ₂ molar ratio for designated surface morphological and compositional types ^a			
	Type 1	Type 2.1	Type 2.2	Type 3
<i>10 nm (analysis beam 10 nm from surface)</i>				
0.5 h				
Surface hydrates	0.25 ± 0.25	0.75 ± 0.25	1.25 ± 0.25	–
3 h				
Surface hydrates	0.45 ± 0.15	0.85 ± 0.15	1.7 ± 0.2	–
Outgrowths	0.35 ± 0.15	0.85 ± 0.10	–	2.0 ± 0.1
7 h				
Surface hydrates	–	0.80 ± 0.15	–	–
Outgrowths	–	0.70 ± 0.10	1.5 ± 0.1	2.1 ± 0.2
<i>40 nm (analysis beam 40 nm from surface)</i>				
0.5 h				
Surface hydrates	–	0.75 ± 0.25	1.2 ± 0.2	–
3 h				
Surface hydrates	–	0.85 ± 0.10	1.5 ± 0.1	2.0 ± 0.4
Outgrowths	0.15 ± 0.15	0.75 ± 0.20	–	1.8 ± 0.2
7 h				
Surface hydrates	–	0.80 ± 0.15	–	–
Outgrowths	–	0.85 ± 0.15	1.3 ± 0.2	1.95 ± 0.15

^a ± values are standard deviations.

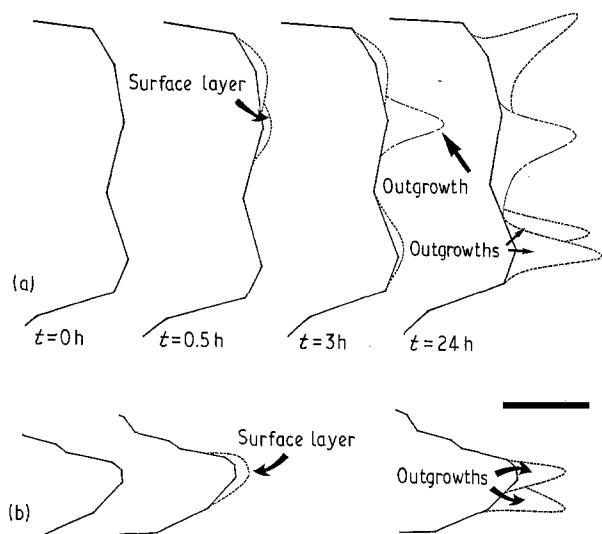


Figure 2 Schematic diagram of development of "surface layers" and "outgrowths" on $3\text{CaO}\cdot\text{SiO}_2$ during the first 24 h hydration. (a) Plan view, (b) side view as imaged in TEM; bar = ca. 200 nm.

view shown is that as imaged in the TEM, whilst information on the idealized side view was obtained by tilting the specimen. The above designations have been used to analyse and collate the wide range of CaO/SiO₂ compositions found at early hydration ages (see Fig. 1). A micrograph of the hydrated "surface layers" after 0.5 h hydration is shown as Fig. 3, whilst micrographs of the two designated microstructural types at 3 h and 7 h are shown as Figs 4 and 5, respectively.

At 0.5 h hydration the surface reactivity of $3\text{CaO}\cdot\text{SiO}_2$ was found to be extremely variable (see Fig. 3). In certain regions significant hydration has occurred, whilst others appear to remain basically anhydrous, at least on the scale of only a few atomic layers of ca. 1 nm. The hydrated "surface layers" were

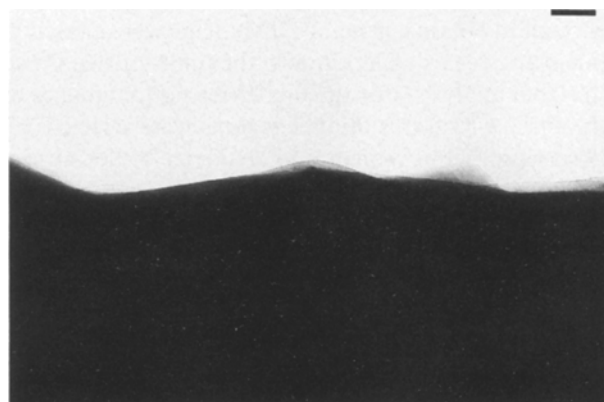


Figure 3 Micrograph of surface features of $3\text{CaO}_2\cdot\text{SiO}_2$ at 0.5 h; bar = 50 nm.

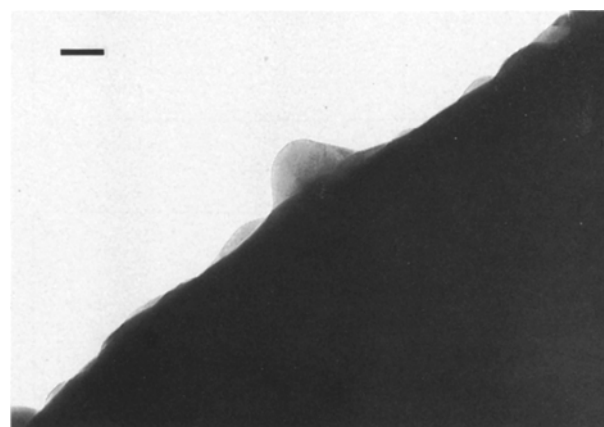


Figure 4 Micrograph of surface features of $3\text{CaO}_2\cdot\text{SiO}_2$ at 3 h; bar = 50 nm.

analysed at 10 and 40 nm designated distances from the film edge and a wide range of CaO/SiO₂ ratios were found (see Fig. 1). Within the first 10 nm the surface composition was found to range from a near

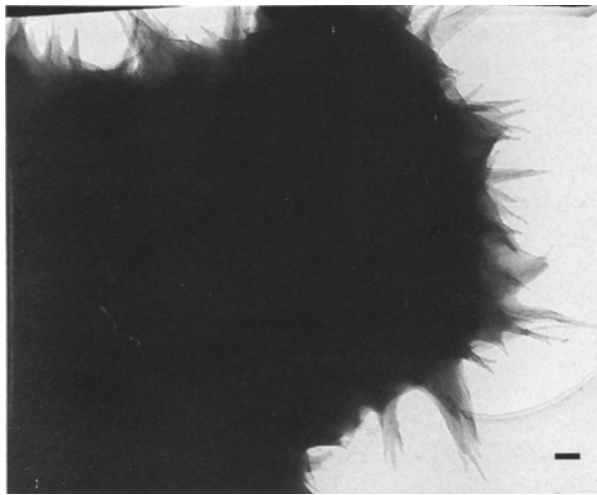


Figure 5 Micrograph of surface features of $3\text{CaO}\cdot\text{SiO}_2$ at 7 h; bar = 100 nm.

CaO-free hydrous SiO_2 to CaO contents somewhat closer to that typically quoted for $1.5\text{CaO}\cdot\text{SiO}_2\cdot x\text{H}_2\text{O}$ [4], and to anhydrous $3\text{CaO}\cdot\text{SiO}_2$. The near CaO-free phase was found to be extremely unstable in the analyser beam and therefore considered to be hydrous silica. On moving the analysis to 40 nm from the film edge (centre at 20 nm) the CaO/SiO₂ compositions were found to be somewhat different (see Fig. 1). Now close to 40% of the analyses are of anhydrous $3\text{CaO}\cdot\text{SiO}_2$, and the hydrous SiO_2 phase is no longer apparent. Using a somewhat arbitrary division of a CaO/SiO₂ ratio of 1 for possible compositional type designation, two hydrate types can perhaps be distinguished. The estimated compositions of these are quoted together with the standard deviations in Table I. The two compositions defined at 0.5 h are 0.75 ± 0.25 and 1.2 ± 0.2 CaO/SiO₂.

At 0.5 h hydration the initial surface hydrolysis reaction therefore occurs at only specific active sites on the $3\text{CaO}\cdot\text{SiO}_2$, whilst other regions remain virtually unaffected. The analytical TEM results are therefore in general accord with thermoluminescence studies by Fierens and Verhaegen [9, 10]. In their investigations the early reaction was found to occur at active sites such as nucleophilic excited centres on the surface. In contrast, our compositional results do not appear to agree with equivalent early hydration studies using surface-sensitive techniques such as XPS and ESCA [11, 12]. For instance, Ménétrier *et al.* [11] found Ca/Si at 0.5 h to be 1.5, close to the CaO/SiO₂ ratio found at later ages. This apparent disagreement between the composition of the surface hydrates is probably related to the low spatial resolution of the techniques used compared to analytical TEM. The values quoted would then comprise not only surface hydrates of lower CaO contents but also unreacted $3\text{CaO}\cdot\text{SiO}_2$, as found in our studies.

At 0.5 h hydration the range of hydrate compositions found, and their overall relatively low CaO content, provides direct experimental evidence at the 10 nm scale of the preferential dissolution of Ca^{2+} ions from the surface layers. In our studies it would

appear that this can proceed as far as hydrous SiO_2 in specific regions. Regourd *et al.* [12] have found a similar overall selective dissolution of Ca^{2+} ions from the surface using XPS; however, the wide range of compositional types observed in our studies would again tend to be averaged out and therefore remain undetected.

At somewhat later ages of 3 h and 7 h similar surface-analytical TEM studies were undertaken. The wide range of compositional data obtained are presented in convenient form in Fig. 1, whilst micrographs of typical hydrated surfaces are shown as Figs 4 and 5. In these, two general surface features were distinguished and designated "surface layers" and "outgrowths" (see Fig. 2). On some of the more reactive $3\text{CaO}\cdot\text{SiO}_2$ grains, considerably more general hydration could be observed (see Fig. 5). In such areas "surface layers" was defined as the valley-like region between the more well-defined "outgrowths".

At 3 h the hydrated "surface layers" analysed at 10 nm from the surface appear to have three reasonably distinct compositions, averaged as 0.45 ± 0.15 , 0.85 ± 0.15 and 1.7 ± 0.2 CaO/SiO₂, (see Table I). Moving further into these layers to 40 nm, the compositions distinguished were 0.85 ± 0.10 , 1.5 ± 0.1 and 2.0 ± 0.4 CaO/SiO₂ (this last almost certainly containing a contribution from $3\text{CaO}\cdot\text{SiO}_2$). The hydrate of unusually low CaO content was no longer found when the deeper "surface layers" were analysed. The "outgrowths" analysed at 10 nm were found to have a similar composition to the "surface layers" (see Table I). At 40 nm the low-CaO hydrate material 0.15 ± 0.15 CaO/SiO₂ still remains in the "outgrowths", in contrast to the "surface layers" at this depth. It is uncertain why this should be so, but a possible explanation is that the relative rates of dissolution of Ca^{2+} ions from the anhydrous $3\text{CaO}\cdot\text{SiO}_2$ could be an important variable. The larger "outgrowths" have a greater relative surface area compared to the surrounding aqueous phase, enabling a greater rate of dissolution compared to the hydrated "surface layers", which are also thinner and therefore nearer to the anhydrous $3\text{CaO}\cdot\text{SiO}_2$.

At 7 h hydration the hydrated "surface layers" were found to have a composition of 0.80 ± 0.15 CaO/SiO₂, whilst the "outgrowths" contain this plus perhaps two additional hydrate compositions of 1.5 ± 0.1 and 1.95 ± 0.15 CaO/SiO₂, (see Table I). The hydrate compositions present at 7 h hydration were found to be basically independent of the TEM analysis depth. At 7 h hydration the very low CaO-containing hydrate is no longer detectable, probably due to diffusion of Ca^{2+} ions into the hydrated surface layers from the aqueous phase [1]. The higher CaO contents of the "outgrowths" compared with "surface layers" would indicate these to be a later stage in the overall hydration process. By more indirect methods Odler and Dörr [26] have also shown the earlier hydrates to have on average lower CaO contents. The CaO/SiO₂ values found in the "outgrowths" are close to those often quoted for the later calcium silicate hydrate formed in the paste hydration of $3\text{CaO}\cdot\text{SiO}_2$ [5].

3.2. Micro and molecular structure of early hydrates

To investigate the character of the developing hydrates in more detail, higher magnification through-focus TEM was undertaken of thin surface features during the first 24 h of hydration. In our previous studies of calcium silicate hydrates formed in model systems the micro and molecular structure was characterized [24]. The structural features found for the calcium silicate hydrate formed in the paste hydration of $3\text{CaO}\cdot\text{SiO}_2$ will be compared and contrasted not only with our earlier studies, but also with other postulated structures for the paste hydrate.

The hydrates being investigated are not unexpectedly beam-sensitive, and therefore only an extremely limited set of successful micrographs were obtained compared to the total. These fortunately cover the period of the analytical TEM studies described previously, plus an additional somewhat later age of 24 h. The low stability of hydrates in the imaging beam has considerably limited the practical resolution achievable, to somewhat grosser molecular features on the 1 nm scale. In spite of this a number of important structural features of the developing hydrates have been identified, enabling comparisons to be undertaken with previous experimental studies [24] and postulated structures [16, 17, 28].

In each of the micrographs shown the overall averaged CaO/SiO_2 composition will be quoted, this being obtained at the end of the through-focus sequence. Due to the high failure rate, more detailed compositional analysis of the imaged microstructural features was not unfortunately possible.

3.2.1. Hydrates formed at 0.5 h

At the earliest hydration age of 0.5 h the optimum through-focus micrograph of typical thin hydrated "surface layers" is shown as Fig. 6. This consists of a basically random array of mainly ca. 1 nm spots, with perhaps some elliptically shaped spots ca. $1\text{ nm} \times 2\text{ nm}$ in size. The generally speckled image observed is typical of amorphous monatomic solids [27]. This particular type of image is difficult to analyse in structural terms, since the detail observed is not only



Figure 6 Micrograph of surface layers ($\text{CaO}/\text{SiO}_2 = 0.8$) at 5 h; bar = 10 nm.

related to the sample itself, but also to various instrumental factors [27]. In spite of this important limitation the speckled image does appear to be related to randomly oriented ca. 1 nm fragments of calcium silicate hydrate. This size is such that they are but tiny fragments of the structure proposed by Ramachandran *et al.* [13] and observed by Henderson and Bailey [24]. These structures are sheet-like in character, with a core layer of protonated CaO_x polyhedra sandwiched between short-chain silicate groups, reminiscent of the layers in crystalline tobermorite [21]. If the image has structural significance, the proposed ca. 1 nm long fragments would represent approximately only one unit cell assembly of lattice ions, if based on a tobermorite-like structure (unit cell $a/2 = 0.558\text{ nm}$, $b = 0.739\text{ nm}$, $c/2 = 1.1389\text{ nm}$ [21]). Instead of the highly orientated two-dimensional structure observed for the calcium silicate hydrate in model systems [24], these are but tiny fragments perhaps $1\text{ nm} \times 1\text{ nm}$ and $1\text{ nm} \times 2\text{ nm}$ in size. This large-scale loss in structural development is perhaps not so surprising, since to actually form this hydrate of averaged composition $0.9\text{ CaO}/\text{SiO}_2$, close to 70% of the CaO in anhydrous $3\text{CaO}\cdot\text{SiO}_2$ must have been removed. This almost certainly occurs by rapid hydrolysis of the Ca^{2+} ions from the surface of the silicate; not only during the initial mixing with water, but also throughout the early part of the dormant period [12]. To form the imaged "surface hydrate" ca. 70% of the Ca^{2+} ions must have been lost from the original anhydrous crystalline metasilicate lattice. It is therefore perhaps not so surprising that this hydrate is not only completely amorphous on the 1 nm scale, but the molecular fragments themselves are short-chained at only 1–2 nm.

3.2.2. Hydrates formed at 3 and 7 h

The optimal through-focus bright-field micrographs of the surface hydrates at the somewhat later ages of 3 and 7 h are shown as Figs 7 and 8, respectively. At 3 h hydration the micrograph shown consists of two typical "outgrowths" as described earlier (see Fig. 7). In general the overall image again consists of a speckled array of spots, similar to that observed at 0.5 h

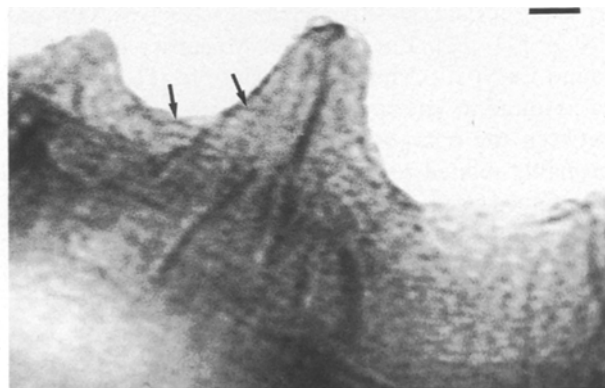


Figure 7 Micrograph of outgrowths ($\text{CaO}/\text{SiO}_2 = 0.9$) at 3 h; bar = 10 nm.

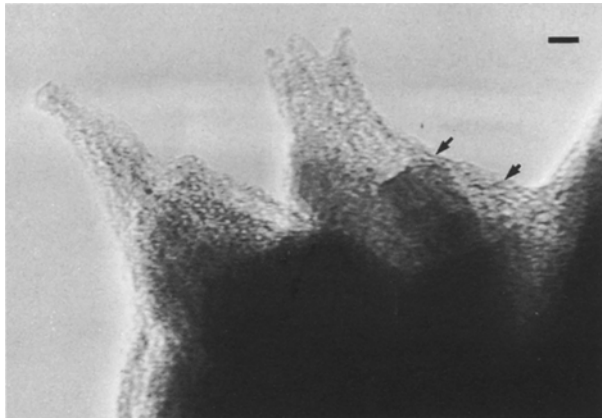


Figure 8 Micrograph of outgrowths ($\text{CaO}/\text{SiO}_2 = 1.2$) at 7 h; bar = 10 nm.

hydration and typical of thin amorphous films. However, in addition to this, there are many ca. 1 nm thick fragments, some ca. 3 nm long and extending for up to ca. 15 nm (see arrowed regions in Fig. 7). The high contrast of these fragments would suggest that they are not filament-like, but instead have, in addition to the observable 1 nm \times 3 nm size, a reasonable extension in the third dimension. These ca. 3 nm long fragments are reasonably straight, and can extend for up to 5–6 units, in what appears to be disjointed steps. Since no continuous extensions of the fragments were observed, as would appear possible (by chance) if the third dimension was large, we tentatively suggest this to be also 3 nm.

The above more organized regions are shown schematically in Fig. 9. These idealized structural representations are of the single ca. 3 nm long fragments and also of the disjointed interconnected segments of the layer-like structure of calcium silicate hydrate, with triangles representing the silicate tetrahedra and the core consisting of protonated CaO_x polyhedra [13, 24]. The interconnections are shown as occurring from the CaO_x polyhedral core to the silicate tetrahedra, as indicated by the disjointed step-like connections imaged (see arrowed regions in Fig. 7). Instead of the curved molecularly continuous sheets extending over some 10^4 – 10^6 nm² observed in model systems by

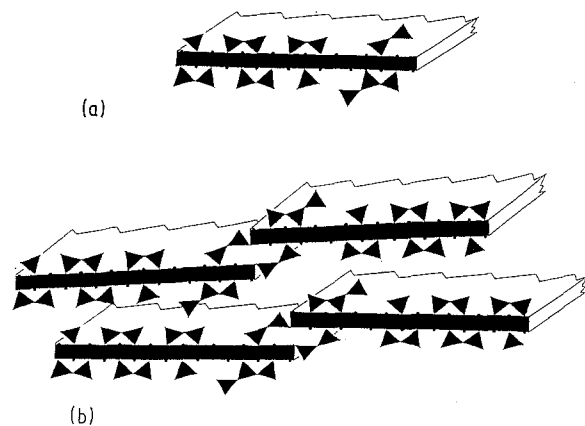


Figure 9 Schematic representation of the layer-like structure of the calcium silicate hydrate: (a) single fragment, (b) disjointed fragments as double layer.

Henderson and Bailey [24], in the paste hydration of $3\text{CaO} \cdot \text{SiO}_2$ the maximal disjointed extension is only 15 nm. This is 1–2 orders of magnitude less, indicating the extremely limited extent of the minimal structural ordering within the early hydrates in $3\text{CaO} \cdot \text{SiO}_2$, compared to those prepared in model systems. In several regions these apparently disjointed 1 nm thick fragments exist as multilayers of the calcium silicate hydrate sheet, close to 1.0–1.5 nm apart with up to four layers in certain areas (see arrows in Fig. 7). These are somewhat reminiscent of the much longer multilayers observed in our earlier studies [24]. The multilayers observed are not, however, parallel over distances greater than approximately 3 nm, the length of the individual calcium silicate hydrate sheet fragments, and even then in only limited regions.

The overall extent of the above tentative structural order is extremely limited, perhaps some 5 nm \times 15 nm in extent before disordering recurs. The actual degree of structural ordering does not appear to be high even in the multilayer regions, and it is therefore doubtful if micro-diffraction would be successful. Unfortunately this interesting though remote possibility was not pursued further, since the hydrates were considered too unstable. The minimal ordering that has been observed occurs near the saddle of the “outgrowth” or on the nearside, possibly indicative of some memory of the dynamic processes leading to the development of this “outgrowth”.

A possible mechanism to describe the development of such “outgrowths” is based on the osmotic semipermeable membrane hypothesis proposed by Birchall *et al.* [29] to explain the early hydration behaviour of $3\text{CaO} \cdot \text{SiO}_2$. In this mechanism, osmosis of the aqueous phase through the semipermeable early surface hydrates occurs throughout the dormant period. This ends when the osmotic pressure bursts the “outgrowths” and then the acceleratory period of the hydration sequence begins.

At 7 h hydration the micrograph shows two typical “outgrowths” described earlier (see Fig. 8). These have a definite appearance of being hollow, especially the wider-topped one consisting of three almost certainly open lips. The uniform contrast throughout at least 50% of this outgrowth provides additional evidence of its hollow character [30]. Such hollow “outgrowths” have been observed previously, but perhaps not so directly [31]. Their existence at the appropriate time provides direct evidence for an osmotic semipermeable membrane type of mechanism, as proposed by Birchall *et al.* [29] to describe the early hydration behaviour of $3\text{CaO} \cdot \text{SiO}_2$. In general the overall impression of this micrograph is of a hydrate which is somewhat less well structurally organized than the previous micrograph obtained at 3 h. This could well be due to the more rapidly occurring dynamic processes occurring during this acceleratory period in the hydration of $3\text{CaO} \cdot \text{SiO}_2$. The probable directly observed rupture of the end of the “outgrowths” is evidence of such dynamic processes. Further away from these, there is some evidence of 1 nm thick fragments of the calcium silicate hydrate layer, some 2 nm long and extending up to ca. 6 nm (see arrows in

Fig. 8). These appear to be similar to those observed at 3 h, although somewhat shorter, and also to schematic representations shown in Fig. 9. At this age the extent of these more structurally organized regions does not appear to be greater than approximately $2\text{ nm} \times 6\text{ nm}$.

3.2.3. Hydrates formed at 24 h

After 24 h hydration the surface of $3\text{CaO} \cdot \text{SiO}_2$ is completely covered by fibril-like "outgrowths" some 170 nm long and 120 nm wide at the base (Fig. 10). It is interesting to note that at this age these "outgrowths" are no longer open as observed at 7 h hydration. Similar general microstructural features of the calcium silicate hydrate at this hydration time have been widely reported [7, 32].

To investigate the structural character of the 24 h hydrate, high magnification through-focus micrographs were obtained. A typical image of the ca. 1 nm detail observable is shown as Fig. 11. In many areas the typical speckled image of amorphous films was again observed, similar to the more disordered regions in the "outgrowths" at earlier ages. However, there are again additional features similar to the more "ordered" regions observed earlier, but at this age they appear to be somewhat more prevalent. In certain regions discrete 1 nm thick calcium silicate hydrate fragments close to 3 nm long can be distinguished (see short arrow in Fig. 11). On the shoulder of the fibril, the 1 nm thick fragments extend for up to ca. 15 nm in a series of disjointed, thread-like growths some 1 nm apart covering a region of approximately $5\text{ nm} \times 15\text{ nm}$. This more structurally "organized" calcium silicate hydrate is also observed to perhaps a more limited extent near the tip of the fibril and nearer the base (see longer arrows in Fig. 11).

3.2.4. Microheterogeneous structure

In the cross-sectional area of the fibril outgrowth described above, the relative proportions of the amorphous to more structurally organized calcium

silicate hydrate was estimated to be as follows:

- (i) completely amorphous ca. 70–80%,
- (ii) 3 nm long discrete fragments ca. 10–20%,
- (iii) structurally more "ordered" regions ca. 10%.

The 3 nm long discrete fragments of the 1 nm thick sheet-like layer are reminiscent of the ca. 6 nm long structural fragments postulated by Taylor [33]. However, in addition to these there are regions where somewhat longer-range incipient order is observed on the $5\text{ nm} \times 15\text{ nm}$ scale. At least at this age the calcium silicate hydrate appears to be structurally heterogeneous on the 1–10 nm scale. The degree of incipient ordering therefore appears to range from amorphous on the 1 nm scale, through small 3 nm long, 1 nm thick individual fragments of the sheet-like structure, similar to that proposed by Taylor [33], to more extensive regions on the $5\text{ nm} \times 15\text{ nm}$ scale. The 3 nm long fragments and the more structurally ordered regions are basically similar to those observed at earlier hydration ages and shown schematically in Fig. 9. The somewhat more extensive incipient ordering of a layer-like hydrate is similar to that proposed by Daimon *et al.* [34]. No experimental evidence was obtained for any of the proposed three-dimensional silicate framework-like structures [16, 17].

It is important to remember not to exaggerate what has been termed longer-range incipient ordering, as implying crystalline order in the conventional sense. We are rather indicating the range of micro-assemblies of the observed fragments of the calcium silicate hydrate sheet, above the completely random level. To investigate in more detail the character of these regions of incipient ordering, techniques such as micro-micro diffraction are of potential value, but unfortunately were not utilized.

The basic 3 nm long and 1 nm thick fragments of the calcium silicate hydrate sheet observed in these investigations are surprisingly close to the ca. 6 nm long fragments postulated by Taylor [33]. The additional extent of the incipient ordering observed in limited regions of these fragments is between one and

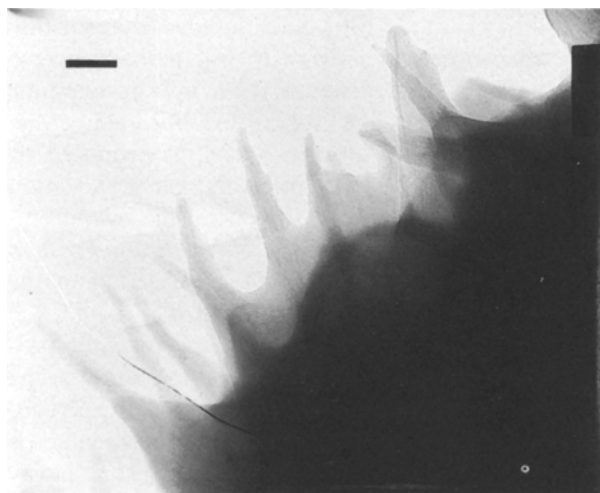


Figure 10 Micrograph of hydrated $3\text{CaO} \cdot \text{SiO}_2$ at 24 h; bar = 50 nm.

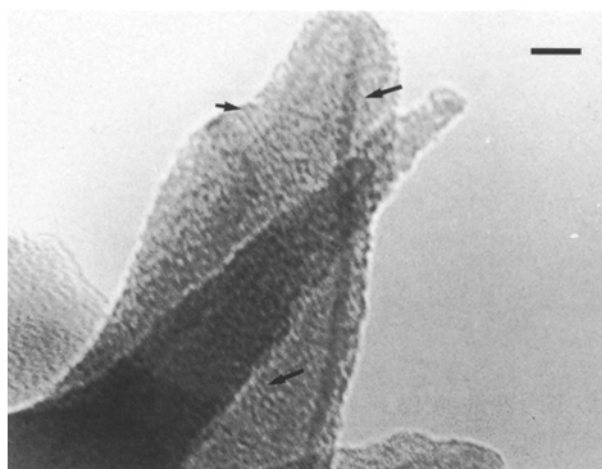


Figure 11 Micrograph of outgrowths ($\text{CaO}/\text{SiO}_2 = 1.5$) at 24 h; bar = 10 nm.

two orders of magnitude less than that observed by Henderson and Bailey [24] in synthetic calcium silicate hydrates formed in model systems. In these the structural 1 nm thick sheet extends continuously for some 10^4 – 10^6 nm, whilst in the paste hydrates even the longer ca. 15 nm fragments are built up from discrete 3 nm segments. The microstructural character of the early paste hydrates at the 1–10 nm scale is therefore somewhat different from that of compositionally similar synthetic hydrates. For the 1–10 nm scale structural characteristics being described, it would appear that the model calcium silicate hydrates studied by Henderson and Bailey [24] are perhaps not that microstructurally close to the $3\text{CaO}\cdot\text{SiO}_2$ paste hydrates, except in retaining the 1 nm thick protonated CaO_x polyhedral layer sandwiched between silicate groups, as shown schematically in Fig. 9.

In all the early hydrates formed at 3 h or more, the basic calcium silicate hydrate structural fragment appears to be close to 3 nm long and 1 nm thick, probably reminiscent of the schematic representation shown in Fig. 9. This appears to be the maximal extent of translational order along the sheet; beyond this, the ordering breaks down completely in most areas of the hydrates, or in certain apparently more ordered regions is at least disjointed. This lack of larger-scale structural ordering is probably related to the increasingly saturated and supersaturated $\text{Ca}(\text{OH})_2$ solution present during the early hydration of $3\text{CaO}\cdot\text{SiO}_2$. This general lack of large-scale structural ordering was found in model studies [24]. In these, the calcium silicate hydrates formed at high $\text{Ca}(\text{OH})_2$ saturation levels were found to be invariably amorphous. However, the 10^2 – 10^3 nm scale microstructural character was similar to that of crystalline hydrates formed at lower $\text{Ca}(\text{OH})_2$ concentrations, so additional micro-environmental factors must therefore also be operating in the two systems. To account for the observed differences in the microstructural characteristics of the hydrates formed, these factors must depend on the mode of formation.

In relation to the tobermorite-like sheet, the maximal translational ordering of ca. 3 nm would represent only four unit cells along the b direction of the orthorhombic unit cell $a = 1.12$, $b = 0.74$, $c = 2.28$ nm as defined by Hamid [21]. The next sheet-like fragment, if present, appears to form a disjointed linkage with the previous fragment, and in relation to the proposed sheet-like structure this occurs via the silicate tetrahedra, rather than continuously through the CaO_x core layer (see Fig. 9). This represents an important molecular structural difference between the more “ordered” regions in these paste hydrates and those observed in model systems [24].

4. Conclusions

The unique ability of TEM has been used to not only characterize the changes in microstructural development of the early hydrates in the $3\text{CaO}\cdot\text{SiO}_2$ – H_2O system, but also to analyse in detail the complex microheterogeneous nature of these amorphous phases. In addition, it has been possible for the first

time to obtain images of the hydrates enabling their molecular character on the 1 nm scale to be identified.

The initial reaction between the $3\text{CaO}\cdot\text{SiO}_2$ surface and water molecules occurs at specific sites only, whilst the remainder can remain unaffected for at least 3 h. At 0.5 h the hydrates observed within the first 10 and 40 nm of the surface have compositions ranging from hydrous silica to $\text{CaO}/\text{SiO}_2 = 1.2$. Analytical TEM has shown not only the importance of specific reactive sites during the early hydration, but also the extent of leaching of Ca^{2+} ions from these centres.

At 3 h hydration a wide range of hydrate compositions were again characterized. In addition to the “surface hydrates” observed previously, an additional microstructural hydrate was distinguished and designated “outgrowths”. These presumably developing due to osmotic forces within the surface hydrate– $3\text{CaO}\cdot\text{SiO}_2$ interface. The two defined microstructural types have, within the first 10 nm from the surface, a similar range of CaO/SiO_2 compositions. These again range from hydrous silica to $\text{CaO}/\text{SiO}_2 = 0.85$ and possibly 2.0 ± 0.1 in the “outgrowths”. At 40 nm from the surface the very low CaO compositional types were either absent or of less relative importance.

At 7 h hydration the two microstructural types are still present. In this, the acceleratory period of the hydration, the “outgrowths” were found to be open-ended and generally hollow. These, in particular, are presumably formed due to the osmotic forces within the surface hydrate– $3\text{CaO}\cdot\text{SiO}_2$ interfacial region bursting the initially sealed “outgrowths”. At 7 h hydration the basic compositional types identified ranged from $\text{CaO}/\text{SiO}_2 = 0.8$ to 2.1. The actual significance of these compositional types is uncertain, but they are probably related not only to the more rapid hydration occurring at this time, and to the interrelated increased rate of dissolution of Ca^{2+} ions from the $3\text{CaO}\cdot\text{SiO}_2$, but also to the crystallization of $\text{Ca}(\text{OH})_2$ which occurs at this stage of the hydration sequence.

The directly observed dynamic changes in the microstructure of the “surface hydrates”, the development and subsequent bursting of the “outgrowths” and the overall changes in the CaO/SiO_2 composition have been explained in relation to the osmotic semipermeable membrane mechanism [35]. In general terms this hypothesis has been found to provide the most satisfactory explanation of the TEM results.

Higher magnification images of the hydrates formed within the first 24 h have for the first time shown not only molecular structural detail at the 1 nm scale, but also their microheterogeneous character at the 1–10 nm scale. At 0.5 h, however, no evidence was observed for the development of any structural identity beyond the ca. 1 nm scale. Instead a randomly speckled image was obtained, consistent with that of an amorphous film. No direct evidence of even limited structural ordering above the ca. 1 nm scale was observed. However, these short fragments possibly represent one unit-cell assembly of lattice ions, if based on a tobermorite-like structure. The rapid loss of Ca^{2+} ions from the surface layers of the $3\text{CaO}\cdot\text{SiO}_2$ up to

this time would not unexpectedly lead to a considerable decrease of structural ordering from that of the original crystalline lattice.

At 3 h hydration and later, the "outgrowths" imaged were found to contain small, somewhat more structurally ordered regions within the generally amorphous hydrate. At 7 h limited evidence was obtained of some loss of this incipient ordering. This is probably due not only to the more rapid dynamic processes occurring in this, the acceleratory period, but also to the disruption caused by the bursting of the "outgrowths", forming the open-ended structures imaged.

In general, all the hydrates formed after 3 h were found to be microheterogeneous consisting of the following:

1. Amorphous regions without discernible structural detail on the 1 nm scale. This represents the most predominant structural type in all of the hydrates studied.

2. The first level of incipient structural ordering, consisting of 1 nm thick, invariably 3 nm long and possibly 3 nm wide fragments of the proposed sheet-like structure for calcium silicate hydrate.

3. The final level of incipient structural ordering, consisting of regions up to 5 nm × 15 nm in size. These appear to consist of disjointed sheets of the 3 nm long calcium silicate hydrate fragments, extending for up to ca. 15 nm in certain hydrates. The disjointed fragments exist not only as single 1 nm thick sheets, but also as multilayers typically ca. 1 nm apart.

The relative proportion of each of the above has been estimated at 70–80%, 10–20% and 10%, respectively, in one particularly microheterogeneous "outgrowth".

The maximal observed translational ordering of the structure of the 1 nm thick sheet-like fragments extends for only 3 nm. The proposed molecular structure of these is based on the sheet-like structure of tobermorite. The 3 nm long fragments would then represent only four unit cells along the *b* direction before structural disordering recurs.

In the more organized ca. 15 nm long fragments the individual segments still remain only 3 nm long, with the disjointed linkage occurring between the silicate tetrahedra and the central CaO_x polyhedral layer, instead of continuously through this sheet. In contrast the model hydrates [24] were found to extend continuously through the CaO_x polyhedral layer for up to 10³ nm, some two orders of magnitude longer than in the paste hydrates.

The microstructural character of the early paste hydrates at the 1–10 nm scale appears to be somewhat different from the compositionally similar hydrates formed in model systems. It is proposed that the above and additional microstructural differences are not only related to the nucleation and growth of disordered lattices in saturated solutions, but also to differences in the micro-environments between the paste and model systems. The 3 nm long sheet-like fragments directly observed are probably more closely related to the structure proposed by Taylor [19]. In addition our studies have also shown the presence of

regions containing more structurally ordered assemblies of these fragments than that postulated.

Acknowledgements

This work was performed in part at the Department of Materials Science and Engineering, University of Surrey, Guildford, Surrey, UK. One of the authors (E. H.) would like to thank Blue Circle Industries PLC, Research Division, Greenhithe, Kent for their permission to participate in the Royal Society/SERC Industrial Fellowship scheme, and also these bodies for their support of these investigations. We would also like to thank our colleagues at Surrey and Sheffield for their help in using the TEM and ancillary equipment etc., and for many useful discussions.

References

1. H. M. JENNINGS, in "Advances in Cement Technology", edited by S. N. Ghosh (Pergamon, London, 1983) p. 349.
2. J. P. SKALNY and J. F. YOUNG, "Mechanisms of Portland Cement Hydration", in Proceedings of 7th International Congress on the Chemistry of Cement, Paris, 1980, Vol. 1 (Septima, Paris, 1980) p. 1113.
3. RILEM Committee 68-MMH, Task Group 3, *Matér Constr.* **17** (1984) 102.
4. H. F. W. TAYLOR in "Cement Chemistry" (Academic, London, 1990) p. 123.
5. *Idem*, "Chemistry of Cement Hydration", in Proceedings of 8th International Congress on the Chemistry of Cement, Rio de Janeiro, 1986, Vol. 1, p. 82.
6. N. L. THOMAS and D. D. DOUBLE, *Cem. Concr. Res.* **11** (1981) 675.
7. H. R. STEWART and J. E. BAILEY, *J. Mater. Sci.* **18** (1983) 3686.
8. P. FIERENS, J. TIRLOCQ and J. P. VERHAEGEN, *Cem. Concr. Res.* **3** (1973) 549.
9. P. FIERENS and J. P. VERHAEGEN, *ibid.* **6** (1976) 103.
10. *Idem*, *ibid.* **5** (1975) 587.
11. D. MÉNÉTRIER, I. JAWED, T. S. SUN and J. SKALNY, *ibid.* **9** (1979) 473.
12. M. REGOURD, J. H. THOMASSIN, P. BAILEY and J. C. TOURAY, *ibid.* **10** (1980) 223.
13. V. S. RAMACHANDRAN, R. F. FELDMAN and J. J. BEAUDOIN, in "Concrete Science: Treatise on Current Research" (Heydon, London, 1981) p. 59.
14. H. F. W. TAYLOR, *Chem. Ind.* (19 September, 1981) 620.
15. J. E. BAILEY and H. R. STEWART, *Proc. Br. Ceram. Soc.* **35** (1984) 193.
16. F. G. R. GIMLETT, Z. MOHM, AMIN and K. S. W. SING, in Proceedings of 7th International Conference on Chemistry of Cement, Paris, 1980 Vol. 2 (Septima, Paris, 1980) p. 11.
17. A. GRUDEM, in Proceedings of RILEM-INSIA Symposium, Toulouse (Cement and Concrete Research Institute, Stockholm, (CBI report 9: 75), 1972) p. 27.
18. S. DIAMOND, in Proceedings of Conference on Hydraulic Cement Pastes; Their Structures and Properties, University of Sheffield (Cement and Concrete Association, UK, 8–9th April, 1976) p. 2.
19. H. F. W. TAYLOR, in Proceedings of 5th International Symposium on Chemistry of Cements, Tokyo, 1968, Vol. 2 (Cement Association of Japan, 1969) p. 1.
20. R. H. SMITH, P. BAYLISS and B. R. GAMBLE, *Cem. Concr. Res.* **2** (1972) 559.
21. S. A. HAMID, *Z. Kristogr.* **154** (1981) 189.
22. H. STADE and W. WIEKER, *Z. Anorg. Allg. Chem.* **466** (1980) 55.
23. H. STADE, *ibid.* **470** (1980) 69.
24. E. HENDERSON and J. E. BAILEY, *J. Mater. Sci.* **23** (1988) 501.

25. H. F. W. TAYLOR, in Proceedings of Engineering Foundation Conference, New Hampshire, 1979, edited by J. Skalny, (Cement Production & Use, Nos. 79-08) p. 107.
26. I. ODLER and H. DÖRR, *Cem. Concr. Res.* **9** (1979) 277.
27. D. J. SMITH, W. O. SAXTON, J. R. A. CLEAVER and C. J. D. CATTO *J. Microsc.* **119** (1) (1980) 19.
28. J. W. JEFFERY, *Acta. Crystallogr.* **5** (1952) 26.
29. J. D. BIRCHALL, A. J. HOWARDS and D. D. DOUBLE, *Cem. Concr. Res.* **10** (1980) 145.
30. P. J. GOODHEW and D. CHESCOE, Institute of Physics Conference Series No. 61 (EMAG, Cambridge, 1981) p. 351.
31. R. D. COATMAN, N. L. THOMAS and D. D. DOUBLE, *J. Mater. Sci.* **15** (1980) 2017.
32. H. M. JENNINGS, B. J. DALGLEISH and P. L. PRATT, *J. Amer. Ceram. Soc.* **64** (1981) 567.
33. H. F. W. TAYLOR, in Proceedings of Engineering Foundation Conference, New Hampshire, 1979 edited by J. Skalny, (Cement Production & Use, Nos. 79-08) p. 113.
34. M. DAIMON, S. A. ABO-EL-ENEIN, G. HOSAKA, S. GOTO and R. KONDO, *J. Amer. Ceram. Soc.* **60** (1977) 110.
35. J. D. BIRCHALL, A. J. HOWARD and J. E. BAILEY, *Proc. Roy. Soc. (London)* **A360** (1978) 445.

*Received 9 October
and accepted 17 November 1992*